A Review, Evaluation, and Correlation of the Phase Equilibria, Heat of Mixing, and Change in Volume on Mixing for Liquid Mixtures of Methane + Ethane

M. J. Hiza, R. C. Miller*, and A. J. Kidnay**

Thermophysical Properties Division, National Engineering Laboratory, National Bureau of Standards, Boulder, Colorado 80303

The available experimental data for liquid-vapor equilibria, heat of mixing, and change in volume on mixing for the methane + ethane system have been reviewed and where possible evaluated for consistency. The derived properties chosen for analysis and correlation were liquid mixture excess Gibbs energies, Henry's constants, and K values. Data sets, selected on the basis of the consistency tests applied, were correlated as functions of temperature and composition to provide internally consistent sets of property values suitable for engineering design calculations.

Key words: Binary mixtures; data correlation; excess volumes; heat of mixing; liquid-vapor equilibria; methane + ethane.

Contents

1. Introduction

Accurate thermodynamic properties for mixtures of cryogenic fluids are necessary for current and proposed industrial applications. Low-temperature processing of gas mixtures containing low-molecular-weight hydrocarbons is increasing. Volumetric (P-V-T-x) data are required to design fluid-handling equipment, custody transfer systems and high-pressure separation processes. Phase equilibria data are necessary for separation equipment design, and enthalpy data are of direct use in heat exchanger design.

Experimental results are particularly important for binary systems, because these data form the basis for multicomponent mixture prediction techniques. Of the possible binary systems, methane + ethane is perhaps the single most important system related to the natural gas industry, and many experimental studies have been made on this system.

A survey of important cryogenic fluid mixtures data prior to January 1, 1975, has been made [1],[1] and a preliminary evaluation of liquid-vapor equilibria data for the methane + low molecular-weight alkane binary systems is also available [2].

The objective of this work is to review, evaluate, and correlate the liquid-vapor equilibria and certain related thermodynamic properties data for the methane + ethane system. The properties chosen for analysis are the excess Gibbs energy, liquid-vapor equilibrium ratio, Henry's constant, excess enthalpy, and excess volume.

2. Review of Phase Equilibria Data

The published liquid-vapor equilibria references for the methane + ethane system are listed in table 1. The tem-

* Department of Mineral Engineering, University of Wyoming.
** Department of Chemical and Petroleum-Refining Engineering, Colorado School of Mines.

[1] Figures in brackets indicate literature references at the end of this paper.

TABLE 1. Survey of liquid-vapor equilibria data for methane + ethane

References	Experimental method	Approximate temperature and pressure ranges [a]	Comments
Uehara (1932) [3]	Static gas solubility measurements	140 to 155 K (1 bar)	Six T-x data points are tabulated at 1 bar total pressure.
Michels and Nederbragt (1939) [4]	Dew and bubble points estimated from compressibility isotherms passing through the two-phase region	273 K (30 to 70 bar)	An approximate P-x-y diagram is presented, based on two dew-point and two bubble-point estimates.
Ruhemann (1939) [5]	Flow method	169 K (1 to 22 bar); 185 K (1 to 41 bar); 195 K (2 to 85 bar); 273 K (27 to 83 bar)	The measured isothermal data are presented only as graphs. A table is given of T-x values at approximately 5, 10, 15 and 20 bar, as calculated from the isotherms.
Guter, Newitt and Ruhemann (1940) [6]	Flow method	195 K (5 to 61 bar)	Revised values are given in tabular form for the 195 K isotherm of Ruhemann (1939).
Levitskaya (1941) [7]	Recirculation	178 K (30 bar); 188 K (30, 41 bar)	The measurements were made on the hydrogen + methane + ethane system, and only three data points are given for the methane + ethane binary.
Bloomer, Gami and Parent (1953); Ellington, Eakin, Parent, Gami and Bloomer (1959) [8]	Dew-point, bubble-point	140 to 300 K (7 to 69 bar)	Both references present the same data. Isothermal P-x-y graphs are given at 172, 200, 233, and 273 K, constructed by cross-plotting the data.
Price and Kobayashi (1959) [9]	Vapor recirculation	172 K (7, 14 bar); 200 K (7, 14, 27, 42 bar); 228 K (14, 27, 144 K (7 bar); 42, 55 bar)	Measurements are reported for the methane + ethane + propane system, including eleven data points for the methane + ethane binary.
Chang and Lu (1967) [10]	Vapor recirculation	122 K (0 to 2 bar); 171 K (3 to 21 bar)	
Skripka, Nikitina, Zhdanovich, Sirotin and Benyaminovich (1970) [11]	Vapor recirculation	123 K (0 to 2 bar); 133 K (0 to 5 bar); 143 K (0 to 8 bar); 153 K (0 to 12 bar)	Liquid compositions and total pressures are reported.
Hsi and Lu (1971) [12]	Vapor recirculation	159 K (2 to 14 bar)	
Wichterle and Kobayashi (1972) [13]	Vapor recirculation	130 K (0 to 4 bar); 144 K (0 to 8 bar); 158 K (0 to 15 bar); 172 K (0 to 25 bar); 186 K (1 to 41 bar); 188 K (32 to 43 bar); 190 K (1 to 45 bar); 191 K (1 to 47 bar); 192 K (2 to 48 bar); 194 K (43 to 49 bar); 195 K (36 to 50 bar) 200 K (2 to 52 bar)	
Wilson (1975) [14]	Static	111 K (0 to 1 bar)	Liquid compositions and total pressures are reported.
Davalos, Anderson, Phelps and Kidnay (1976) [15]	Vapor recirculation	250 K (13 to 67 bar)	
Miller and Staveley (1976) [16]	Static	116 K (0 to 1 bar)	Liquid compositions and total pressures are reported.
Miller, Kidnay and Hiza (1977) [17]	Vapor recirculation	160 K (0 to 13 bar); 180 K (1 to 28 bar)	

[a] 1 bar = 10^5 pascal = 0.986923 atmosphere.

perature and pressure ranges are given for all data, along with the methods of measurement and comments concerning the type of data presented.

Wilson [18] has recently reviewed the techniques commonly used for low-temperature liquid-vapor equilibria measurements. Recent measurements for methane + ethane have been by either the static method (at low pressures) or the vapor recirculation method (at moderate to high pressures). The choice of method relates to both ease of operation and accuracy of the results.

The static method is particularly well suited to low-pressure measurements for methane + ethane (temperatures below 130 K). The liquid composition is usually determined by adding known amounts of the pure components to the equilibrium cell, and correcting for the amount of material in the vapor phase. This procedure is often more accurate than liquid sampling and analysis. Generally only one datum point is obtained for each charge to the cell. Only a small correction need be applied for the amount of material in the vapor phase, which is predominantly methane, and the gas-phase nonideality corrections are small and can be estimated easily. A suitable method is then used to accurately calculate gas-phase compositions from the isothermal P-x data, such as those of Barker [19]; Van Ness, Byer and Gibbs [20]; or Christiansen and Fredenslund [21].

The vapor recirculation system is popular for moderate to high pressures because of its versatility and reliability. Only a modest amount of material is required, and equilibrium is easily attained. With care, representative samples can be withdrawn and analyzed, although sampling becomes difficult at pressures below 1 bar. Wide ranges of temperature and pressure may be studied without changes in technique. The cell may also be made visual for studies with more than one liquid phase and for studies near the mixture critical locus.

3. Pure Fluid Properties

Accurate pure fluid properties data are necessary in the application of most consistency tests and are often useful in determining whether a set of experimental data suffers from temperature or pressure measurement errors or sample impurities.

Fortunately, for both methane and ethane, the thermodynamic properties have been recently evaluated and correlated by Goodwin [22,23], and the results are available in both equation and tabular form. The critical properties of the pure components as listed in references [22] and [23] are:

CH_4 $T_c = 190.555$ K
$P_c = 45.988$ bar
$V_c = 100$ cm³/mol
C_2H_6 $T_c = 305.33$ K
$P_c = 48.715$ bar
$V_c = 147$ cm³/mol

Vapor pressures from all studies are compared with Goodwin [22,23] in table 2. There are no large discrepan-

TABLE 2. Comparison of experimental (EXPR) vapor pressures (bar) with those listed in compilations (COMP)

	Methane			Ethane			
T, K	EXPR	COMP [a]	Δ, %	EXPR	COMP [b]	Δ, %	Reference
110.93	0.965	0.956	0.9				Wilson [14]
115.77	1.4034	1.4065	0.2				Miller and Staveley [16]
122.04	2.23	2.21	0.9	0.005	0.0047	6	Chang and Lu [10]
123.15	2.38	2.38	0.0	0.005	0.0055	9	Skripka et al. [11]
130.37	3.72	3.76	1.1	0.0129	0.0135	4.4	Wichterle and Kobayashi [13]
133.15	4.42	4.42	0.0	0.02	0.0186	7	Skripka et al. [11]
143.15	7.52	7.53	0.1	0.05	0.0521	4	Skripka et al. [11]
144.26	7.85	7.95	1.3	0.0580	0.0579	0.2	Wichterle and Kobayashi [13]
153.15	11.95	11.98	0.2	0.13	0.1259	3	Skripka et al. [11]
158.15	14.69	14.79	0.7	0.1871	0.1868	0.2	Wichterle and Kobayashi [13]
160.00				0.2173	0.2146	1.3	Miller et al. [17]
171.43	24.70	24.53	0.7				Chang and Lu [10]
172.04	24.93	25.07	0.6	0.4895	0.4884	0.2	Wichterle and Kobayashi [13]
186.11	39.92	40.03	0.3	1.103	1.101	0.2	Wichterle and Kobayashi [13]
189.65	44.68	44.71	0.1	1.325	1.324	0.1	Wichterle and Kobayashi [13]
190.94	46.25	[c]		1.407	1.412	0.4	Wichterle and Kobayashi [13]
192.39				1.520	1.527	0.5	Wichterle and Kobayashi [13]
199.92				2.168	2.167	0.0	Wichterle and Kobayashi [13]
250.00				13.02	13.01	0.1	Davalos et al. [15]

[a] Reference [22].

[b] Reference [23].

[c] Reference [22] gives the critical temperature of methane as 190.555 K.

cies from which definite conclusions can be drawn concerning impurity or temperature scale and pressure problems. If reported, the actual experimental vapor pressures were used in all evaluation work reported here. If experimental vapor pressures were not reported the values were taken from Goodwin.

4. Evaluation of Experimental Data

Evaluation or consistency testing of experimental data may be divided into three general categories: internal consistency tests which measure the scatter or imprecision of a single set of measurements, mutual consistency tests which seek to intercompare data from different sources, and thermodynamic consistency tests which attempt to assess the correspondence of a given set of experimental measurements to known thermodynamic relations. It is desirable to use tests from all three categories for data evaluation, but often it is difficult or impossible to do so. The variety of experimental methods and the range of operating conditions encountered in experimental measurements generally make it impossible to apply only a single test from each category to all the data for one system.

A description of the major categories of experimental liquid-vapor equilibria data, along with a brief discussion of the types of consistency tests presently available for these data, will serve to illustrate the problems faced by the evaluator. Liquid-vapor equilibria data are usually found in one of three forms: 1) isothermal measurements of P-x-y, 2) isothermal measurements of P-x, with y being obtained by computation, and 3) measurements of dew and bubble points for mixtures of constant composition. In each category a further subdivision of the data may occur between low- and moderate-pressure regions where both components are subcritical, and high pressure regions where one component is supercritical.

Graphical evaluations of the data, such as plots of (y_1P/P^s_1) versus P, (K_1P) versus P, and x_2 versus $(P\text{-}P^s_1)$ not only provide an excellent assessment of scatter among data points, but also provide a check on the temperature and pressure measurements and material purity. For the first two tests, as the system pressure (P) approaches the vapor pressure of component 1 (P^s_1), the term (y_1P/P^s_1) must extrapolate smoothly to unity, and the term (K_1P) must extrapolate smoothly to (P^s_1). These tests may be applied to dew- and bubble-point data only by extensive crossplotting with resultant loss of accuracy, and any graphical construction involving y is inapplicable to isothermal P-x data. It is generally assumed that the authors have performed these simple graphical tests. These methods were not directly employed in this work, but the equivalent of these tests is included in the work done here.

Thermodynamic consistency tests are usually based on the Gibbs-Duhem equation, but these tests take a variety of forms. The most widely used are discussed by Prausnitz [24], Van Ness [25] and Van Ness, Byer, and Gibbs [20]. Unfortunately, most thermodynamic consistency tests are limited to the low-pressure region where deviations from ideal vapor-phase behavior are either negligible or small. The usefulness of one of the most widely used procedures, the equal areas test, has been seriously questioned recently [20]. A technique that has been used extensively in recent years is the calculation of y from P-T-x data, and the comparison of the calculated y values with those obtained experimentally. The works of Barker [19] and Christiansen and Fredenslund [21] are examples of this method. The evaluation of data at high pressures involves the introduction of an empirical equation of state, which normally contains several adjustable coefficients that must themselves be obtained from experimental data, and the interpretation of the test results is thus often open to question.

It is apparent from the preceding discussion that the evaluation of all the phase equilibria data for any binary system is not an easily defined task leading to clear-cut conclusions. It is a process requiring some subjective judgments by the evaluator as to the applicability and interpretation of the various consistency tests.

For purposes of evaluation, the methane + ethane data were put into two broad categories using a temperature of 0.9 $(T_c)CH_4$ as the approximate dividing line. The different tests that were applied to the data in the two temperature regions are discussed in the following sections.

4.1. Low-Temperature Phase Equilibria

At temperatures where only low and moderate pressures are encountered gas-phase nonidealities are not difficult to determine, liquid-phase properties are nearly independent of pressure, and liquid-phase activity coefficient behavior is easy to model using the symmetric convention. The typical upper temperature limit for such behavior occurs at a reduced temperature of about 0.9 for the more-volatile component. For the methane + ethane system this temperature is 172 K. Twelve of the fifteen references listed in table 1 present data at 172 K or below.

Initial screening of the data below 172 K was accomplished by intercomparison of the molar excess Gibbs energies (G^E). Parrish and Hiza [2] used the orthogonal collocation method [21] to determine G^E for the experimental isotherms below the methane critical temperature and presented a plot of the equimolar-mixture G^E values versus temperature. A similar plot has been presented [17] based on Barker-method calculations [19]. These graphs indicate that there are a number of experimental isotherms in the 110 to 190 K range which yield equimolar G^E values consistent within about $\pm$ 20 J/mol. However, there are several isotherms which yield G^E values considerably outside this band. Ten isotherms below 172 K were selected by this technique for correlational purposes. One of these isotherms was later excluded from correlation development because of excessive scatter in the data. The remaining nine isotherms are indicated in figure 1, where the equimolar G^E/T values at zero pressure derived from a Barker-

method calculation (cf., Appendix A) are shown versus reciprocal temperature.

The Barker-method calculations (Appendix A) were used to obtain smooth G^E values for the individual isotherms and to test for thermodynamic consistency where possible. The virial equation truncated after the second virial coefficient was used to describe the gas phase, and three-term Redlich-Kister equations were used to represent the composition dependence of G^E at zero pressure. The Redlich-Kister coefficients determined by least-squares fitting of the P-x data are given in table 3. Standard deviations are listed for each coefficient, along with average deviations between calculated and experimental P and y (where measured). For some of these isotherms the standard deviation in the C term was larger than the value of the coefficient, but the coefficients have been retained in the table. Two isotherms (115.77 K and 171.43 K) stand out as having greatly different precision levels from the rest of the data. The 171.43 K isotherm was not included in any correlation work because of the poor precision level. Since only the 115.77 K isotherm had a precision level significantly higher than the rest, it was decided not to use relative weighting factors in correlating the data.

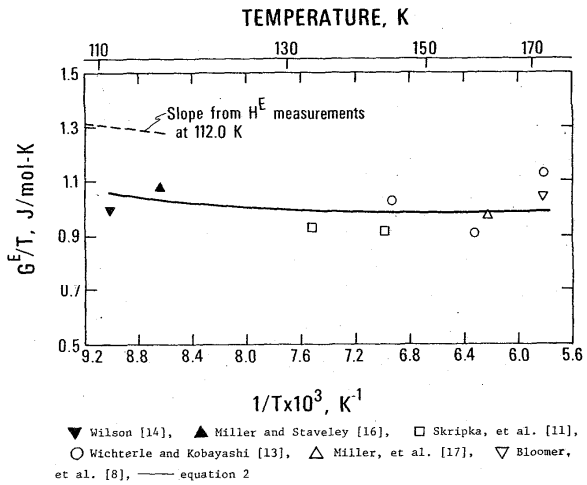

FIGURE 1. Excess Gibbs energies (G^E) at zero pressure as a function of temperature for equimolar liquid mixtures of methane + ethane, determined by the Barker-method analysis of Appendix A.

Except for the 171.43 K isotherm, all data for which measured y values were reported appear to be thermodynamically consistent. Deviations between experimental and calculated y values are on the order of the uncertainties in the composition determinations.

The Barker-method calculations were repeated using the Peng-Robinson equation of state (described in a later section) instead of the truncated virial equation to calculate gas-phase fugacity coefficients. No significant differences were observed between the two methods. Maximum discrepancies in the equimolar G^E values were approximately 3 J/mol.

Of the nine isotherms represented in figure 1, only the four from references [13] and [17] are direct isothermal measurements of P, x and y. The equal areas test was applied to these four isotherms by plotting $ln\ (\gamma_1/\gamma_2)$ against x_1. Activity coefficients were calculated at zero reference pressure using equations A1, A2, A12, and A14, with the data sources listed in Appendix A. The Peng-Robinson equation of state was used to estimate gas phase fugacity coefficients. Results of the test were that the difference of the absolute values of the positive and negative areas divided by the sum of those absolute values ranged from 0.2 to 0.4. From the literature it is unclear whether these values are near enough to zero for the data to be considered thermodynamically consistent. Deviations from ideality are small for methane + ethane, and activity coefficients are generally less than 1.5, thus making an accurate determination of $ln\ (\gamma_1/\gamma_2)$ difficult. Relatively small errors in the data

TABLE 3. Redlich-Kister coefficients from the Barker-method analyses of the individual selected isotherms

CH_4 (1) + C_2H_6 (2)

$$G^E = x_1x_2[A + B(x_1 - x_2) + C(x_1 - x_2)^2]$$

	Coefficients, J/mol			Average Deviations		
T,K	A	B	C	$(\lvert\Delta P\rvert/P^s_1) \times 100$	$\lvert\Delta y_1\rvert$	Reference
110.93	443.4 ± 20[a]	38.8 ± 27[a]	10.5 ± 45[a]	0.49[b]		Wilson [14]
115.77	496.1 ± 2	100.6 ± 3	29.3 ± 4	0.04		Miller and Staveley [16]
133.15	496.5 ± 35	194.4 ± 48	172.1 ± 72	0.47		Skripka et al. [11]
143.15	526.8 ± 35	213.9 ± 49	125.6 ± 74	0.32		Skripka et al. [11]
144.26	611.5 ± 15	174.9 ± 23	59.8 ± 35	0.18	0.0009[c]	Wichterle and Kobayashi [13]
158.15	577.5 ± 17	296.4 ± 29	−26.5 ± 45	0.29	0.0018	Wichterle and Kobayashi [13]
160.00	621.1 ± 12	236.9 ± 20	24.0 ± 31	0.28	0.0007	Miller et al. [17]
171.43	678.3 ± 113	281.8 ± 162	392.7 ± 217	1.12	0.0115	Chang and Lu [10]
172.04	761.3 ± 30	288.5 ± 45	142.4 ± 68	0.39	0.0016	Wichterle and Kobayashi [13]
172.04	720.9 ± 11	317.2 ± 15	132.5 ± 22	0.08	0.0053	Bloomer et al. [8]

[a] Standard deviations in the coeffiicents.

[b] Average absolute deviations between calculated and experimental pressures as a percentage of the methane vapor pressure.

[c] Average absolute deviations between calculated and experimental methane vapor mole fractions.

or in the calculated gas-phase fugacity coefficients will result in considerable discrepancies in the equal areas test.

4.2. High-Temperature Phase Equilibria

Two methods were used to evaluate the liquid-vapor equilibria data at temperatures above 170 K. The orthogonal collocation technique, as described by Christiansen and Fredenslund [21], was used to calculate y values and Henry's constant from the experimental P-x data along each isotherm. A comparison of calculated and experimental y values constitutes a form of thermodynamic consistency test [20,21,26]. The method of Gunn, Yamada and Whitman [27] was also used to intercompare the Van Laar constants for ethane-rich liquid mixtures and to extract Henry's constants. Both calculational methods are documented in Appendix B.

Consistency Testing With the Gibbs-Duhem Equation

Average absolute deviations are given in table 4 between experimental y values and those calculated by the numerical method of orthogonal collocation. Data in the critical region were not included for temperatures of 199.82 K and higher, because the calculated y values for methane invariably became much larger than experimental values in this region. The greatest discrepancy always occurred at the critical point, if this point was reported. Arbitrarily, all data with liquid compositions within 10 mole percent of the critical composition were not included in the averages. According to Christiansen and Fredenslund [21], if the gas-phase equation of state is entirely adequate, the deviations $|\Delta y|$ should not exceed the combined uncertainties in the experimental composition measurements ($\Delta x + \Delta y$). For data of good quality, this experimental uncertainty should not exceed 0.006; however, at the higher temperatures shown in table 4 there may be some uncertainty introduced through use of the modified Redlich-Kwong equation for the gas phase. Even so, average $|\Delta y|$ values should not greatly exceed 0.010 at temperatures above 200 K. Most of the isotherms are consistent within the indicated limits, the most notable exceptions being the isotherms from the early work of Ruhemann [5].

TABLE 4. Results of the orthogonal collocation and Gunn et al. methods

T, K	Orthogonal collocation [21]		Method of Gunn et al. [27]		Data reference
	Avg$\lvert\Delta y_1\rvert$	H_{12}, bar [e]	H_{12}, bar [e]	A, mol/cm^3	
171.43	0.011[a]	31.2[b]			Chang and Lu [10]
172.04	0.006	24.1			Bloomer et al. [8]
172.04	0.002	23.1			Wichterle and Kobayashi [13]
173.15	0.014	31.1			Ruhemann [5]
180.00	0.002	32.9			Miller et al. [17]
183.15	0.017	39.8			Ruhemann [5]
186.11	0.003	33.5	34.0[b]	0.0028[c]	Wichterle and Kobayashi [13]
189.65	0.003	34.4	36.9	0.0031	Wichterle and Kobayashi [13]
190.94	0.005	38.2	37.9	0.0034	Wichterle and Kobayashi [13]
192.39	0.008	36.6	38.7	0.0036	Wichterle and Kobayashi [13]
193.15	0.017	51.3			Ruhemann [5]
199.82	0.011	46.4			Price and Kobayashi [9]
199.82	0.006	46.2	45.0[d]	0.0044[d]	Bloomer et al. [8]
199.92	0.006	41.3			Wichterle and Kobayashi [13]
203.15	0.016	66.6			Ruhemann [5]
213.15	0.022	74.9			Ruhemann [5]
227.59	0.011	72.3	70.3	0.0057	Price and Kobayashi [9]
233.15	0.011	69.2	74.5	0.0054	Bloomer et al. [8]
250.00	0.009	86.9	91.2	0.0060	Davalos et al. [15]
273.15	0.006	98.1	105.2	0.0058	Bloomer et al. [8]

[a] These are the average absolute deviations between calculated and experimental y values for methane. No data points were included with liquid compositions within ten mole percent of the critical composition.

[b] The numbers in these columns are Henry's constants at the ethane vapor pressure.

[c] These numbers are the Van Laar constants as described in reference [27].

[d] These results represent an average arrived at by simultaneous consideration of data from all three data references [8,9,13].

[e] 1 bar = 10^5 pascal = 0.986923 atmosphere.

Evaluation of Henry's Law Constant

Henry's constants are reported in table 4 from both orthogonal collocation [21] and the method of Gunn et al. [27]. The former method uses a numerical extrapolation technique, whereas, the latter method requires evaluator judgment in using a graphical extrapolation procedure. A Henry's law plot of the isotherms considered using the method of Gunn et al. is shown in figure 2. Straight lines were drawn after consideration of all the data on this diagram. This method yields Henry's constants (as infinite dilution intercepts) which show a relatively smooth dependence on temperature. The resulting Henry's constants are plotted versus temperature in figure 3. They were fit by least-squares at temperatures up to 250 K by the equation

$$H_{12} = -132.5 + 0.8916\,T \qquad (1)$$

with a standard deviation of 0.2 bar. Equation (1) is shown as the solid line up to 250 K on figure 3. The dashed curve is from the correlation of Singh and Mukhopadhyay [28].

Also shown in figure 3 are the Henry's constants from the orthogonal collocation program. They are generally in good agreement with the results obtained using the method of Gunn et al., however, they are more scattered. This arises because only data for an individual isotherm were considered in the calculation. Small systematic experimental errors at the most dilute compositions can result in an extrapolated Henry's constant which may not be the best choice. This can be clearly seen for the 233.15 K and 250.00 K isotherms (cf., figure 2), where the collocation method yields results below those obtained graphically.

The method of Gunn et al. also yields a Van Laar constant for each isotherm, which describes liquid-phase activity coefficient behavior. These Van Laar constants are presented in table 4.

Critical Locus Evaluation

The available critical locus data are shown in figure 4. There is good agreement between the data of Bloomer et al. [8] and Wichterle and Kobayashi [13]. Reasonable curves were drawn through these data. No attempt was made to fit these data to particular functional forms.

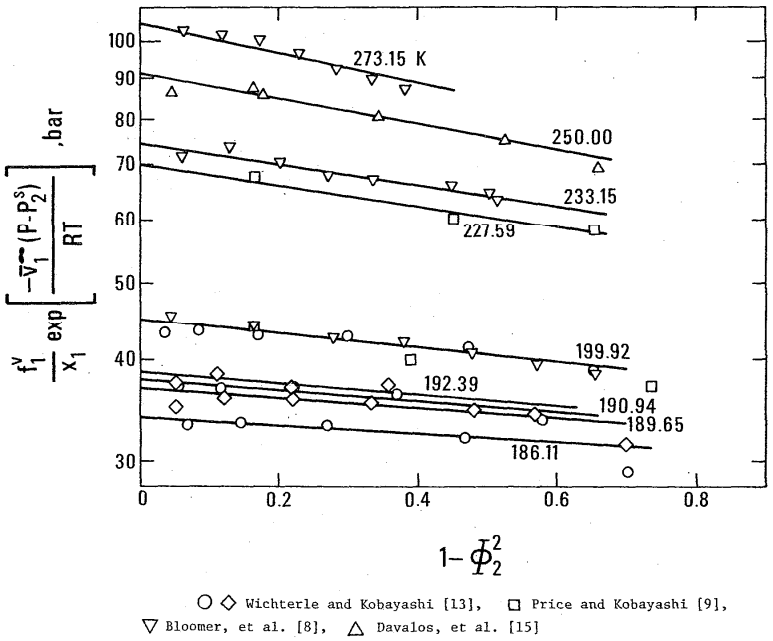

FIGURE 2. Henry's law plot as proposed by Gunn et al. [27] for methane dissolved in liquid ethane, where component 1 is methane. The lines were estimated as those best representing a smooth family for all isotherms shown. The intercepts are Henry's constants (H_{12}) at the pure ethane vapor pressure and the slopes are the Van Laar constants (A) times the partial molar volumes ($\bar{V}_1^{\infty}$).

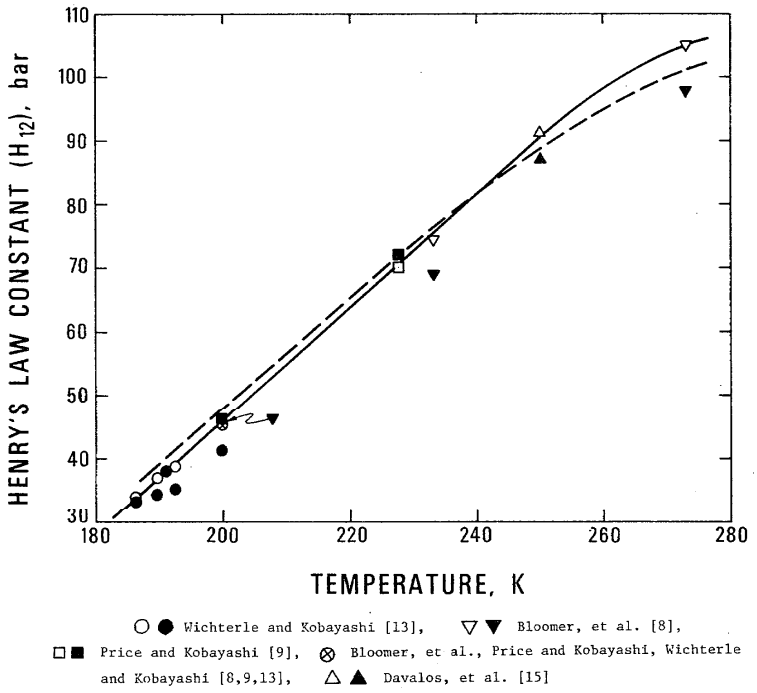

FIGURE 3. Henry's constants (H_{12}) at the pure ethane vapor pressure versus temperature for methane + ethane. Open symbol data were determined by the method of Gunn et al. [27], and the closed symbol data were found by orthogonal collocation [21]. The solid curve is a fit of the open-symbol data (equation (1) below 250 K), and the dashed curve is from Singh and Mukhopadhyay [28].

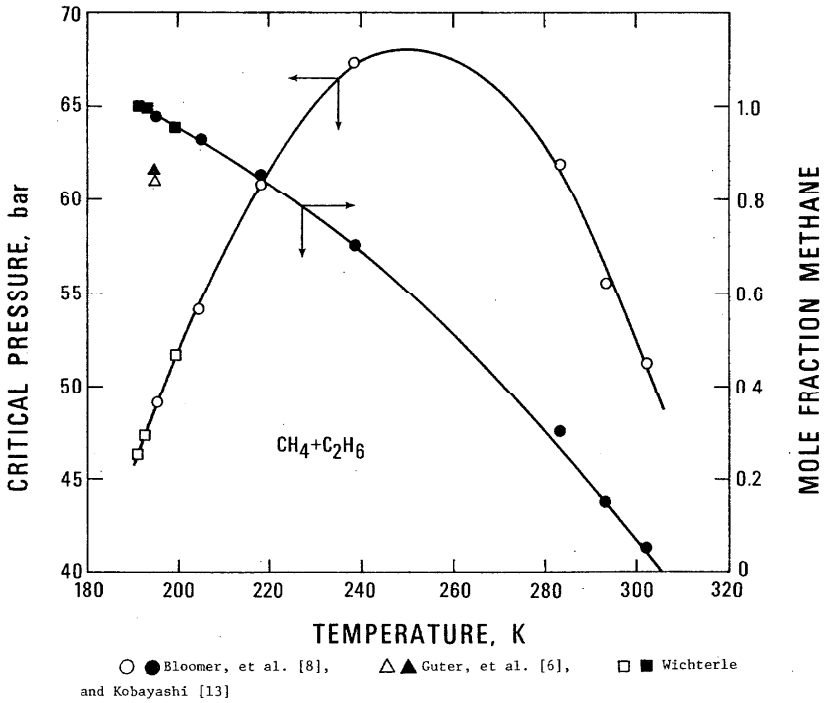

FIGURE 4. Critical pressure and critical mole fraction of methane versus temperature for methane + ethane. Solid curves are estimated best fits of the limited data.

4.3. Volume Change on Mixing and Heat of Mixing (Excess Enthalpy)

Excess volumes for methane + ethane have been reported by several investigators [35-38]. The only methods available for testing this type of data are the graphing of V^E versus composition to evaluate internal scatter, and comparison of midpoint V^E values versus temperature. These methods were used to intercompare the available data, and a correlation of V^E is presented in a later section.

Since only one set of H^E values is available [16], no comparisons are possible.

5. Correlation

5.1. Liquid-Vapor Equilibria

There are a number of methods which can be used to calculate liquid-vapor equilibria for mixtures of low-molecular-weight alkanes over wide ranges of conditions, including the high-pressure region. These methods generally require one or more binary interaction parameters for their application. They might better be called correlational methods than predictive methods when applied to binary systems. Most of the calculational methods can be categorized as 1) a liquid-phase activity coefficient model combined with a gas-phase equation of state, 2) a corresponding states technique, or 3) the use of an equation of state for both phases.

Typical of the first method is the work of Prausnitz and Chueh [29], for which there has been additional correlational work for light-hydrocarbon systems by Singh and Mukhopadhyay [28]. A dilated Van Laar model is used to describe liquid-phase activity coefficients, and a modified Redlich-Kwong equation of state is employed for the gas-phase fugacity coefficients and liquid-phase volumetric behavior.

One of the most sophisticated of the corresponding states approaches has been successfully applied to phase equilibria and other thermodynamic properties of systems containing low-molecular-weight alkanes and nitrogen by Mollerup and Rowlinson [30]. This method is of the conformal solution type, employing pure methane as the reference fluid for which accurate P-V-T properties are assumed known.

Equation of state approaches have become quite popular in the chemical process industry because of the relative ease and speed of computer calculations. Equations of state with the least number of parameters have an inherent advantage in this regard over those with large numbers of coefficients. However, the latter are generally more accurate in their description of pure-component properties and may provide a stronger basis for multi-property mixture work. Typical of this work is the procedure of Han and Starling [31] using a modified Benedict-Webb-Rubin equation of state. The simpler equations have found applicability for specific purposes, such as the calculation of liquid-vapor equilibrium ratios (K values) for natural gas type systems. Many of these calculational schemes employ modified Redlich-Kwong equations, a recent version being due to Peng and Robinson [32]. Three parameters are required for each pure component, although the equation of state is applied to mixtures as if it were a two-constant equation.

In this work the low-temperature methane + ethane phase equilibria data were correlated through the liquid-phase excess properties G^E and H^E combined with a virial equation of state for the gas phase, while the high-temperature data were correlated with the Peng-Robinson equation of state. The use of different equations of state for the two temperature regions was dictated by ease of computer programming, and does not represent a judgement regarding the applicability of the equations in different temperature ranges. The results of these calculations were then combined into a single K-factor chart covering the entire temperature region.

Excess Properties (G^E, H^E)

Excess enthalpy (H^E) data is a valuable tool in correlating G^E data, but the only available data are those of Miller and Staveley [16] who list H^E as a function of composition at 91.5 and 112.0 K. The form chosen for G^E at zero pressure is

$$G^E = x_1 x_2 \sum_{i=0}^{2} \sum_{j=0}^{2} a_{ij} T^j (x_1 - x_2)^i, \qquad (2)$$

which is a three-term temperature dependent Redlich-Kister equation with coefficients quadratic in temperature. The corresponding equation for H^E at zero pressure is

$$H^E = \left[\frac{\partial G^E}{\partial 1/T}\right]_{P,x} = x_1 x_2 \sum_{i=0}^{2} \sum_{j=0}^{2} a_{ij} (1-j) T^j (x_1 - x_2)^i. \qquad (3)$$

Values of G^E at each reported liquid composition for the nine selected isotherms (the isotherms of table 3 with the exception of 171.43 K) were fitted simultaneously with the H^E data by minimizing the unweighted objective function

$$Y \cong \sum_{\substack{\text{LVE data} \\ \text{points}}} (G^E_{CALC} - G^E_{EXPR})^2 + \sum_{\substack{H^E \text{ data} \\ \text{points}}} (H^E_{CALC} - H^E_{EXPR})^2. \qquad (4)$$

Weighting the H^E data more heavily than the G^E data produced an inferior correlation, since the H^E data were all at the lower end of the temperature range. The resulting coefficients a_{ij} are given with their standard deviations in table 5. The C term in the Redlich-Kister equation (given at any temperature by the last three a terms) is retained even though the standard deviation is of the same order as the coefficient. All of the selected isotherms (table 3) with one exception indicate a positive C term. Standard deviation from the 89 combined experimental G^E and H^E values was 8.4 J/mol, with the maximum deviation of 18 J/mol occurring for a G^E value at 172.04 K and a methane mole fraction near 0.32. The solid line in figure 1 was

calculated from equation (2). Root-mean-square deviation between equation (3) and the 11 experimental H^E values was 7.4 J/mol.

Other forms were chosen for G^E and H^E in an attempt to find a correlation. Equations due to Wilson [33] and Liebermann and Fried [34] were used to correlate the selected G^E and H^E data. In both cases standard deviations from the experimental values were considerably larger than standard deviations reported above for equation (2).

TABLE 5. Coefficients for temperature-dependent Redlich-Kister equation determined by simultaneous fit of selected G^E and H^E data

$$CH_4\ (1) + C_2H_6\ (2)$$

$$G^E = x_1x_2 \sum_{i=0}^{2} \sum_{j=0}^{2} a_{ij}\, T^j\, (x_1 - x_2)^i$$

Coefficient	Value [a]	Standard deviation [a]
a_{00}	587.69	50
a_{01}	− 4.0935	0.96
a_{02}	0.027364	0.0042
a_{10}	337.01	112
a_{11}	− 5.6654	2.10
a_{12}	0.032180	0.0091
a_{20}	289.69	305
a_{21}	− 5.6884	5.35
a_{22}	0.026933	0.0223

Standard Deviation in G^E and H^E = 8.40 J/mol.

[a] Units are such that G^E is in J/mol with T in kelvins.

Comparisons have been made between the calculated and the experimental isotherms. When calculating liquid-vapor equilibria using equation (2), the same gas-phase equation of state and data should be used as indicated in Appendix A. Bubble point pressures were calculated for comparison with the experimental isotherms for which y values were not measured. For comparison with the P-x-y measurements, x-y values and K values were calculated at the experimental pressures. The comparisons are given in table 6 and figures 5, 6 and 7. Generally, the calculated and experimental bubble point pressures agree within ± 1% and the mole fractions within ± 0.006 for the isotherms on which the correlation was based (upper part of table 6 and figures 5 and 6). Calculated K values for methane averaged 1.5% different from experiment for these isotherms, while the average deviation for the ethane K values was 5%. Average deviations for all properties were much larger for the isotherms not used in the correlation (lower part of table 6 and figure 7).

Representation of the excess Gibbs energies (G^E) is given by equation 2 and table 5, as derived from a simultaneous fit of selected G^E data and the available H^E data. For mixtures in the mid range of compositions, the absolute uncertainty in the G^E values from the equation is estimated to be about 5 J/mol at 110 K, rising to about 20 J/mol at 172 K. The larger uncertainty at the higher temperatures is due to use of the truncated virial equation of state in arriving at the G^E values, restricting the temperature dependence of G^E to a quadratic form, greater scatter in the phase-equilibria data, and the lack of H^E data at temperatures above 112 K.

Curves are shown in figure 8 of G^E at zero pressure versus composition at 110, 140 and 170 K, as calculated from equation (2). For comparison, G^E values were calculated at 110 and 140 K from an equation by Miller and Staveley [16]. This latter equation was based only on the low-temperature G^E and H^E data of reference [16]. The

TABLE 6. Comparison of bubble point pressures and y-x values between correlation and experiment

	Average deviations [a]						
T, K	$(\lvert\Delta P\rvert/P^s_1) \times 100$	$(\Delta P/P^s_1) \times 100$	$\lvert\Delta x_1\rvert$	Δx_1	$\lvert\Delta y_1\rvert$	Δy_1	Reference
110.93 [b]	1.02	−0.95					Wilson [14]
115.77 [b]	0.21	0.19					Miller and Staveley [16]
133.15 [b]	0.88	0.39					Skripka et al. [11]
143.15 [b]	0.65	0.23					Skripka et al. [11]
144.26 [b]			0.0046	−0.0046	0.0011	0.0011	Wichterle and Kobayashi [13]
158.15 [b]			0.0048	0.0029	0.0013	0.0013	Wichterle and Kobayashi [13]
160.00 [b]			0.0036	0.0016	0.0006	0.0003	Miller et al. [17]
172.04 [b]			0.0066	−0.0060	0.0024	0.0024	Wichterle and Kobayashi [13]
172.04 [b]			0.0033	−0.0033	0.0056	0.0056	Bloomer et al. [8]
123.15 [c]	3.66	−3.12					Skripka et al. [11]
153.15 [c]	1.64	−1.12					Skripka et al. [11]
122.04 [c]			0.0945	−0.0945	0.0011	0.0011	Chang and Lu [10]
130.37 [c]			0.0150	−0.0150	0.0004	0.0004	Wichterle and Kobayashi [13]
159.21 [c]			0.0190	−0.0190	0.0018	0.0018	Hsi and Lu [12]
171.43 [c]			0.0214	−0.0049	0.0116	0.0095	Chang and Lu [10]

[a] All deviations are "experimental" minus "calculated." Subscript 1 refers to methane.

[b] Isotherms used in developing the correlation of equations 2, 3 and table 5.

[c] These isotherms were not used in developing the correlation.

agreement between G^E values from the two equations is within about 5 J/mol between 110 K and 140 K.

TABLE 7. Coefficients for temperature-dependent Redlich-Kister equation determined by fit of H^E data

$$CH_4\ (1) + C_2H_6\ (2)$$

$$H^E = x_1x_2\,[(A_0 + A_1T) + (B_0 + B_1T)\,(x_1 - x_2)]$$

Coefficient	Value [a]	Standard deviation [a]
A_0	658.57	27
A_1	− 3.4311	0.26
B_0	232.69	90
B_1	− 1.8753	0.90

Standard deviation in H^E = 1.97 J/mol.

[a] Units are such that H^E is in J/mol with T in kelvins.

Equation 3 gives a representation of the excess enthalpy (H^E) data, as derived from the simultaneous fits to G^E and H^E data, but this equation does not represent the H^E data within their estimated accuracy. A direct least-squares fit of the zero pressure H^E data at 91.5 K and 112.0 K from Miller and Staveley [16] yields the results shown in table 7. Curves from this equation at 91 K and 110 K are shown in figure 8. A two-term Redlich-Kister equation was used, since the accuracy of the data does not justify more terms. The coefficients were taken to be linear in temperature because there are data for only two isotherms. The standard deviation between the calculated and experimental H^E values is 2.0 J/mol, which is within the estimated experimental uncertainty of 3.0 J/mol.

Equation of State

The Peng-Robinson equation of state was used to correlate the liquid-vapor equilibria data for the methane + ethane system. Somewhat different mixing rules were employed than given in the original reference. These rules and other documentation concerning the calculations are given in Appendix C. Two mixing-rule deviation parameters were determined by optimizing the fit of calculated y and x values to selected experimental results along isotherms. Some data points very close to the mixture critical points were not used in the optimization scheme. For 140 data points on the 16 selected isotherms between 144 K and 273 K, the average absolute deviation in the K values was 2% for methane and 5% for ethane. Comparisons between calculated and experimental data are shown in figures 6 and 9.

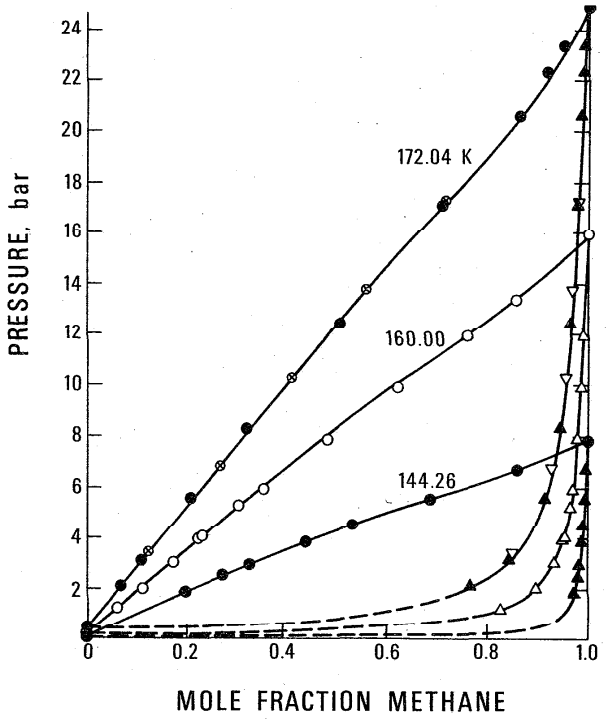

● ▲ Wichterle and Kobayashi [13], ⊗ ▽ Bloomer, et al. [8], ○ △ Miller, et al. [17]

FIGURE 5. Isotherms in the low-temperature region for methane + ethane. Pressure is plotted versus both liquid and vapor mole fractions of methane. The solid curves are based on equation (2) and the method described in section 5.1.

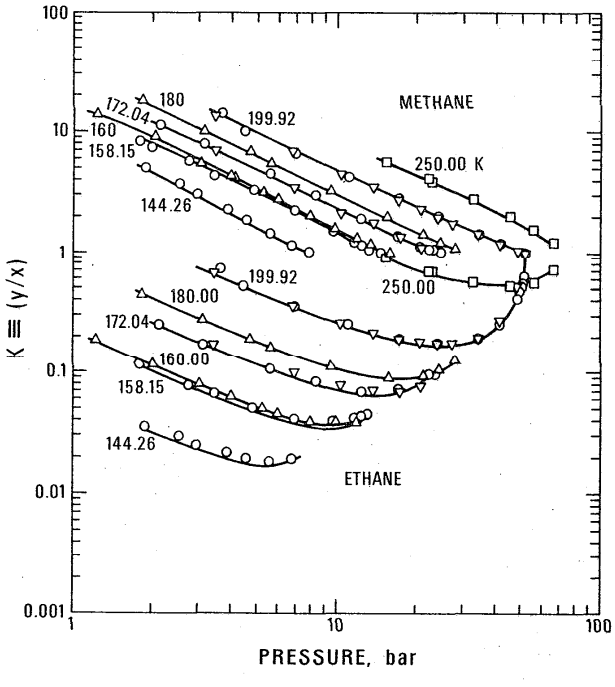

○ Wichterle and Kobayashi [13], △ Miller, et al. [17], ▽ Bloomer, et al. [8], □ Davalos, et al. [15]

FIGURE 6. K values (equilibrium ratios of gas-phase mole fraction y to liquid-phase mole fraction x) for methane and ethane versus pressure for isotherms of methane + ethane. The solid curves at 172.04 K and lower temperatures are from equation (2) and the method described in section 5.1; while the solid curves for 180.00 K and above are from the Peng-Robinson equation of state, as described in section 5.1.

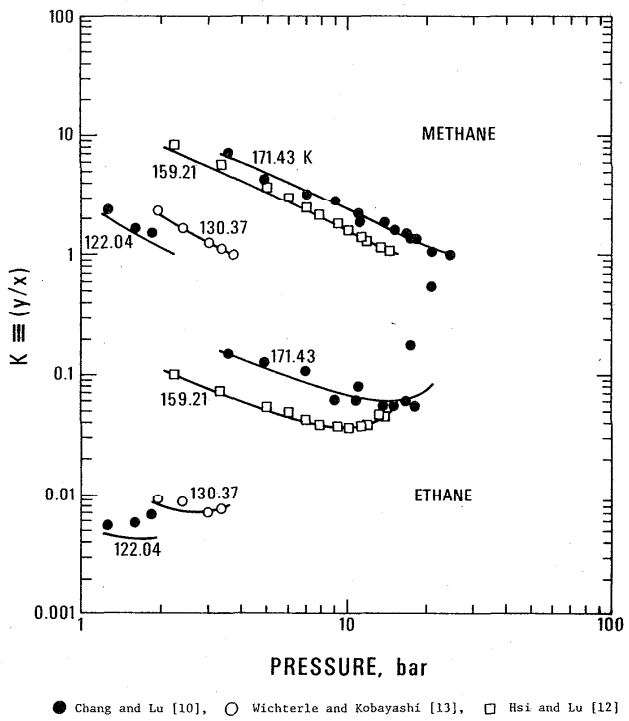

FIGURE 7. K values versus pressure for isotherms of methane + ethane. The solid curves are from equation (2) and the method described in section 5.1.

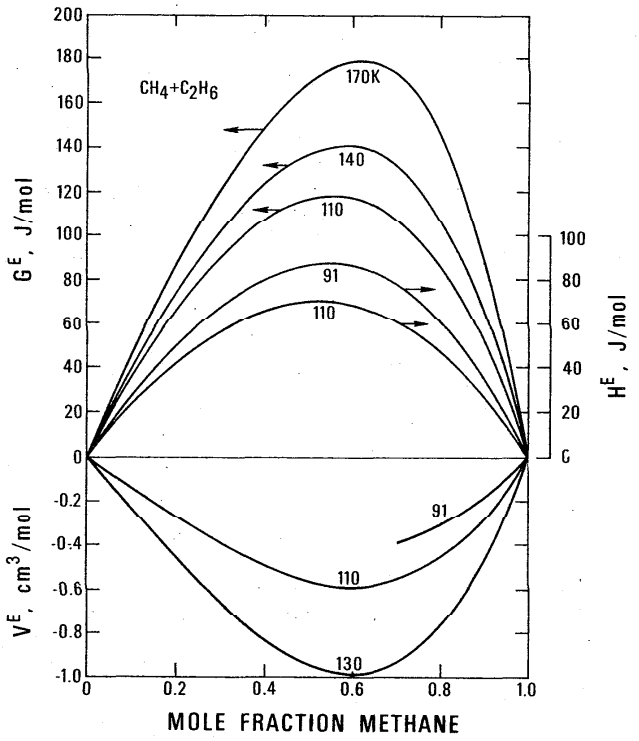

FIGURE 8. Excess Gibbs energies (G^E) at zero pressure from equation (2), excess enthalpies (H^E) at zero pressure from table 7 and excess volumes (V^E) from table 8 versus liquid mole fraction methane for methane + ethane along various isotherms.

K Value Chart

Four sources of information were combined to produce the K-values for methane + ethane presented in figure 10. Vapor pressures were taken from Goodwin [22,23]. Below 172 K, the K-value calculational method described in section 4a was used. This method is based on using a Redlich-Kister equation for the liquid-phase activity coefficients and the truncated virial equation of state for gas-phase nonidealities. Above 172 K, calculations were made as described above, based on use of the Peng-Robinson equation of state for both phases. The mixture critical points were taken from figure 4.

The K-value chart spans the temperature range from 110 K to 250 K with pressures from 0.01 bar up to the maximum mixture critical pressure of 68 bar. It is believed that the accuracy of the ethane K-values is on the same order as the chart can be read, which is about ± 5%. The methane K-values should be as accurate as they can be read from the chart.

5.2. Excess Volume (V^E)

Volumetric data for methane + ethane have been reported by several investigators [1]. Saturated liquid V^E data were reported in references [35-38] between 91 K and 140 K and were fit by least squares to a two-term Redlich-Kister equation with coefficients quadratic in temperature. The results are given in table 8. The standard deviation between calculated and experimental V^E is 0.02 cm³/mol and the maximum deviation is 0.06 cm³/mol for the 50 data points. There is overlap and good agreement among all the data sets. The data do not justify a third term in the Redlich-Kister equation, and addition of such a term does not improve the standard deviation. Excess volumes from the fitting equation, combined with pure-component molar volumes from Goodwin [22,23], should yield methane + ethane liquid mixture molar volumes between 91 K and 140 K accurate to approximately 0.1%.

Curves from the equation in table 8 are presented in figure 8 at 91 K, 110 K and 130 K as V^E versus mole fraction methane. The differences between V^E at zero pres-

TABLE 8. Coefficients for temperature-dependent Redlich-Kister equation determined by fit of V^E data

$$CH_4\ (1) + C_2H_6\ (2)$$

$$V^E = x_1x_2[(A_0 + A_1T + A_2T^2) + (B_0 + B_1T + B_2T^2)(x_1 - x_2)]$$

Coefficient	Value [a]	Standard deviation [a]
A_0	-12.169	2.0
A_1	0.23143	0.033
A_2	- 0.0012838	0.00014
B_0	4.862	4.8
B_1	- 0.07304	0.083
B_2	0.0001802	0.00035

Standard Deviation in V^E = 0.020 cm³/mol.

[a] Units are such that V^E is in cm³/mol when T is in kelvins.

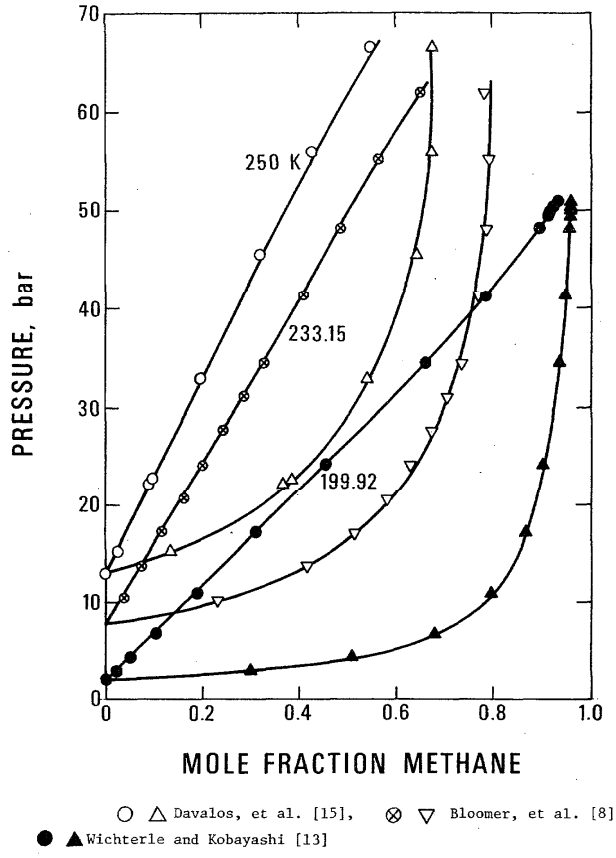

FIGURE 9. Isotherms in the high-temperature region for methane + ethane. Pressure is plotted versus both liquid and vapor mole fractions of methane. The solid curves are from the Peng-Robinson equation of state as described in section 5.1.

sure and V^E at the mixture saturation pressures are less than 0.01 cm^3/mol for temperatures of 130 K or less.

6. Summary

Table 9 lists the liquid-vapor equilibria data found to be consistent using the criteria discussed in the preceding sections. At temperatures below 172 K these data are represented by the Redlich-Kister equation of table 5 for the liquid phase and the virial equation of state through the second virial coefficient for the vapor phase (Appendix A). Above 172 K the data are correlated using the Peng-Robinson equation of state (Appendix C.). The K-value chart of figure 10 provides a convenient summary of the phase equilibria over the entire temperature region of interest.

G^E values extracted from the selected phase-equilibria data below 172 K are fit by the Redlich-Kister equation of table 5. The only available data for the heat of mixing [16] are consistent with the temperature dependence of the selected G^E data and are well represented by the Redlich-Kister equation of table 7. The excess volume data from references [35-38] are consistent and are adequately correlated by a two-term Redlich-Kister equation, table 8.

TABLE 9. Summary of recommended liquid-vapor equilibria data

T, K	Data reference
110.93	Wilson [14]
115.77	Miller and Staveley [16]
133.15	Skripka et al. [11]
143.15	Skripka et al. [11]
144.26	Wichterle and Kobayashi [13]
158.15	Wichterle and Kobayashi [13]
160.00	Miller et al. [17]
172.04	Wichterle and Kobayashi [13], Bloomer et al. [8][a]
180.00	Miller et al. [17]
186.11	Wichterle and Kobayashi [13]
189.65	Wichterle and Kobayashi [13]
190.94	Wichterle and Kobayashi [13]
192.39	Wichterle and Kobayashi [13]
199.82	Price and Kobayashi [9], Bloomer et al. [8][a]
199.92	Wichterle and Kobayashi [13]
227.59	Price and Kobayashi [9]
233.15	Bloomer et al. [8][a]
250.00	Davalos et al. [15]
273.15	Bloomer et al. [8][a]

[a] These isotherms were obtained by cross-plotting of the original dew-point, bubble-point data.

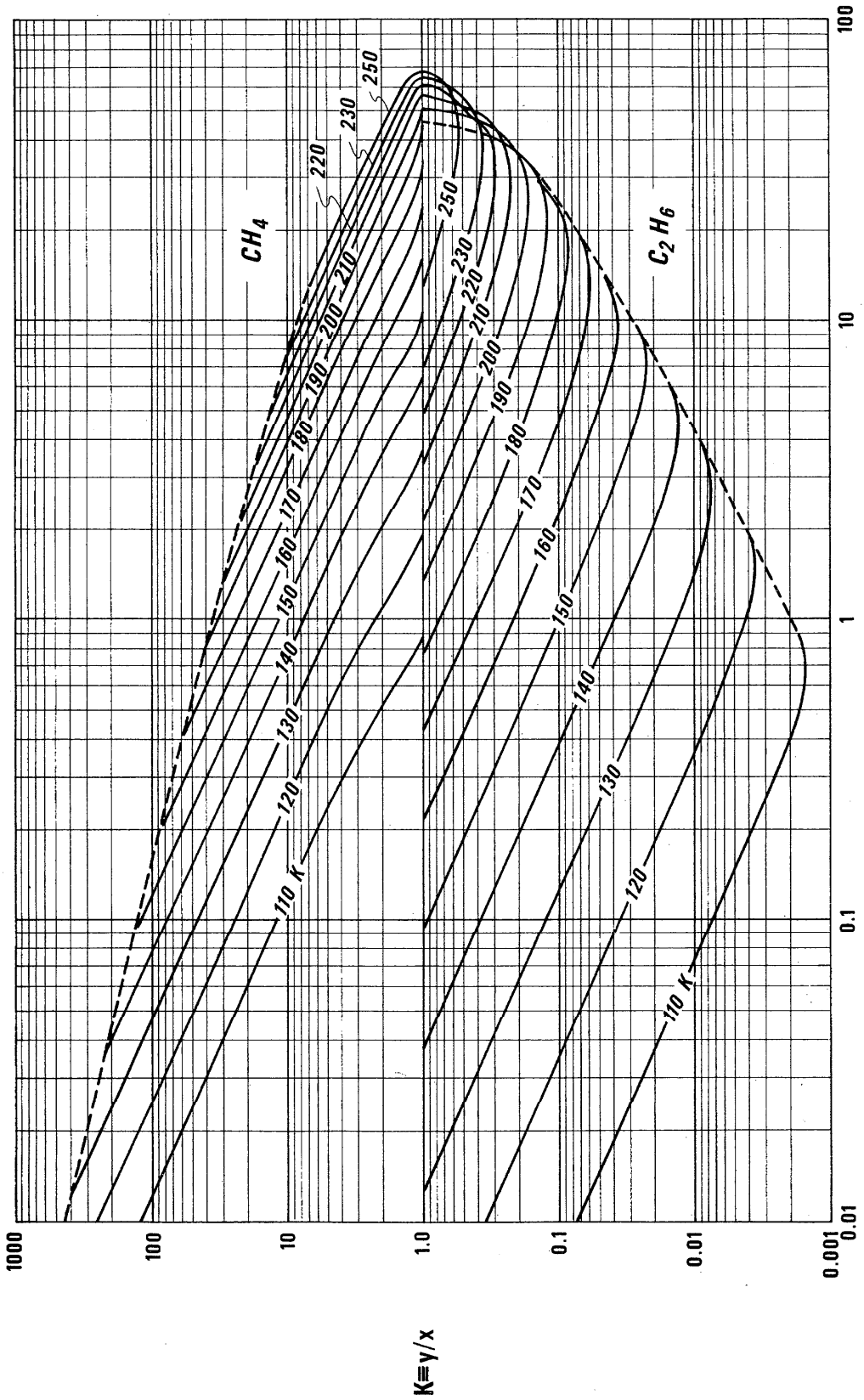

FIGURE 10. K values (y/x) versus pressure along isotherms for methane and ethane in the methane + ethane system.

Acknowledgments

The orthogonal collocation computer program and some of the calculated results therefrom were supplied by W. R. Parrish, National Bureau of Standards. Data fits for the Wilson and Liebermann-Fried equations were done by S. P. Singh, Mineral Engineering Department, University of Wyoming. Financial support for this work was provided by the Office of Standard Reference Data, National Bureau of Standards.

Notation

Symbols

A	=	Van Laar constant, mol/cm³
A''	=	constant in equation A13
A',B',C'	=	constants in equation A11
A_0,A_1,A_2, B_0,B_1,B_2	=	Redlich-Kister coefficients (tables 3,7,8)
a, b	=	equation-of-state constants (Appendix C) or constants in equations A9, A10
c	=	constant in equations A9, A10
B	=	second virial coefficient, cm³/mol
f	=	fugacity, bar
G^E	=	excess Gibbs energy, J/mol
H_{12}	=	Infinite dilution Henry's constant, bar
H^E	=	excess enthalpy or heat of mixing, J/mol
j_{12}, k_{12}	=	equation-of-state interaction constants (Appendix C), dimensionless
K	=	y/x
P	=	pressure, bar
R	=	gas constant
T	=	absolute temperature, K
V	=	molar volume, cm³/mol
V^E	=	excess volume, cm³/mol
$\bar{V}$	=	partial molar volume, cm³/mol
$\bar{V}_1^{\infty}$	—	partial molar volume of component 1 at infinite dilution, cm³/mol
x	=	liquid mole fraction
Y	=	objective function defined by equation 4
y	=	vapor mole fraction
Z	=	PV/RT
a	=	coefficients in the temperature-dependent Redlich-Kister expressions (equations 2 and 3, table 5)
β	=	isothermal compressibility
σ	=	standard deviation
Φ	=	volume fraction, dimensionless
ϕ	=	fugacity coefficient, dimensionless

Subscripts

1	=	methane
2	=	ethane
c	=	critical
i	=	component i

Superscripts

(P^r)	=	evaluated at the reference pressure, $P^r = 0$
S	=	saturation conditions
V	=	vapor

References

[1] Hiza, M. J., Kidnay, A. J., and Miller, R. C., *Equilibrium Properties of Fluid Mixtures: A Bibliography of Data on Fluids of Cryogenic Interest*, NSRDS Bibliographic Series, IFI/Plenum, New York (1975).
[2] Parrish, W. R., and Hiza, M. J., in *Adances in Cryogenic Engineering*, Vol. 21, 485 (Plenum Press, New York, 1976).
[3] Uehara, K., Nippon Kagaku Zasshi. **53,** 931 (1932).
[4] Michels, A., and Nederbragt, G. W., Physica **6,** 656 (1939).
[5] Ruhemann, M., Proc. Roy. Soc. (London) **A171,** 121 (1939).
[6] Guter, M., Newitt, D. M., and Ruhemann, M., Proc. Roy. Soc. (London) **A176,** 140 (1940).
[7] Levitskaya, E. P., Zh. Tekh. Fiz. **11,** 197 (1941).
[8] Bloomer, O. T., Gami, D. C., and Parent, J. D., Inst. of Gas Technol. Res. Bull. No. 22 (1953); Ellington, R. T., Eakin, B. E., Parent, J. D., Gami, D. C., and Bloomer, O. T., *Thermodynamic and Transport Properties of Gases, Liquids, and Solids*, Am. Soc. Mech. Eng. Heat Transfer Div., McGraw-Hill, New York, 180 (1959).
[9] Price, A. R., and Kobayashi, R., J. Chem. Eng. Data **4,** 40 (1959).
[10] Chang, S.-D. and Lu, B. C.-Y., Chem. Eng. Progr. Symp. Ser. **63,** No. 81, 18 (1967).
[11] Skripka, V. G., Nikitina, I. E., Zhdanovich, L. A., Sirotin, A. G., and Benyaminovich, O. A., Gazov. Prom. **15,** No. 12, 35 (1970).
[12] Hsi, C., and Lu, B. C.-Y., Can. J. Chem. Eng. **49,** No. 1, 140 (1971).
[13] Wichterle, I., and Kobayashi, R., J. Chem. Eng. Data **17,** 9 (1972).
[14] Wilson, G. M., in *Advances in Cryogenic Engineering*, Vol. 20, 164 (Plenum Press, New York, 1975).
[15] Davalos, J., Anderson, W. R., Phelps, R. E., and Kidnay, A. J., J. Chem. Eng. Data **21,** 81 (1976).
[16] Miller, R. C., and Staveley, L. A. K., in *Advances in Cryogenic Engineering*, Vol. 21, 493 (Plenum Press, New York, 1976).
[17] Miller, R. C., Kidnay, A. J., and Hiza, M. J., J. Chem. Thermodyn. **9,** 167 (1977).
[18] Wilson, G. M., in *Advances in Cryogenic Engineering*, Vol. 20, 244 (Plenum Press, New York, 1975).
[19] Barker, J. A., Australian J. Chem. **6,** 207 (1953).
[20] Van Ness, H. C., Byer, S. M., and Gibbs, R. E., A.I.Ch.E. J. **19,** 238 (1973).
[21] Christiansen, L. J., and Fredenslund, A., A.I.Ch.E. J. **21,** 49 (1975).
[22] Goodwin, R. D., The Thermophysical Properties of Methane, from 90 to 500 K at Pressures to 700 Bar, Nat. Bur. Stand. (U.S.), Tech. Note 653 (1974).
[23] Goodwin, R. D., Roder, H. M., and Straty, G. C., Thermophysical Properties of Ethane, from 90 to 600 K at Pressures to 700 Bar, Nat. Bur. Stand. (U.S.), Tech. Note 684 (1976).
[24] Prausnitz, J. M., *Molecular Thermodynamics of Fluid-Phase Equilibria*, Prentice-Hall, Englewood Cliffs, New Jersey (1969).
[25] Van Ness, H. C., *Classical Thermodynamics of Non-Electrolyte Solutions*, Macmillan, New York (1964).
[26] Won, K. W., and Prausnitz, J. M., Ind. Eng. Chem. Fundam. **12,** 459 (1973).

[27] Gunn, R. D., Yamada, T., and Whitman, D., A.I.Ch.E. J. **20**, 906 (1974).
[28] Singh, S. P., and Mukhopadhyay, P. K., A.I.Ch.E. J. **18**, 1171 (1972).
[29] Prausnitz, J. M., and Chueh, P. L., *Computer Calculations for High-Pressure Vapor-Liquid Equilibria*, Prentice-Hall, Englewood Cliffs, New Jersey (1968).
[30] Mollerup, J., and Rowlinson, J. S., Chem. Eng. Sci. **29**, 1373 (1974); Mollerup, J., in *Advances in Cryogenic Engineering*, Vol. 20, 172 (Plenum Press, New York, 1975).
[31] Starling, K. E., and Han, M. S., Hydrocarbon Processing **5**, 129 (1972); **6**, 107 (1972).
[32] Peng, D.-Y., and Robinson, D. B., Ind. Eng. Chem. Fundam. **15**, 59 (1976).
[33] Wilson, G. M., J. Amer. Chem. Soc. **86**, 127 (1964).
[34] Liebermann, E., and Fried, V., Ind. Eng. Chem. Fundam. **11**, 350 (1972).
[35] Shana'a, M. Y. and Canfield, F. B., Trans. Faraday Soc. **64**, 2281 (1968).
[36] Rodosevich, J. B., and Miller, R. C., A.I.Ch.E. J. **19**, 729 (1973).
[37] Pan, W. P., Mady, M. H., and Miller, R. C., A.I.Ch.E. J. **21**, 283 (1975).
[38] Hiza, M. J., Haynes, W. M., and Parrish, W. R., J. Chem. Thermodyn. **9**, 873 (1977).
[39] McGlashan, M. L., and Potter, D. J. B., Proc. Roy. Soc. (London) **A267**, 478 (1962); McGlashan, M. L., and Wormald, C. J., Trans. Faraday Soc. **60**, 646 (1964).
[40] Powell, M. J. D., The Computer Journal **7**, 155 (1965).
[41] Dantzler, E. M., Knobler, C. M., and Windsor, M. L., J. Phys. Chem. **72**, 676 (1968).
[42] Hoover, A. E., Nagata, I., Leland, T. W., Jr., and Kobayashi, R., J. Chem. Phys. **48**, 2633 (1968).
[43] Michels, A., and Nederbragt, G. W., as reported by Guggenheim, E. A. and McGlashan, M. L., Proc. Roy. Soc. (London) **A206**, 448 (1951).

Appendix A. Barker-Method Calculations for CH_4 (1) + C_2H_6 (2) Along Isotherms Below 172 K

From the equality of component fugacities in the equilibrium vapor and liquid phases, the symmetric-convention form of the phase equilibrium relation can be written as

$$P y_i \phi_i = f_{\text{pure } i}^{(P^r)} \quad \gamma_i^{(P^r)} \quad x_i \exp \int_{P^r}^{P} \frac{\overline{V}_i dP}{RT}, \qquad \text{(A1)}$$

where,

$$f_{\text{pure } i}^{(P^r)} = P^s{}_i \phi^s{}_i \exp \int_{P^s{}_i}^{P^r} \frac{V_i dP}{RT}. \qquad \text{(A2)}$$

The assumptions utilized in applying equation (A1) in the present work were as follows:

1. The density form of the virial equation of state, truncated after the second virial coefficient term, can be used to calculate fugacity coefficients for pure gases ($\phi^s{}_i$) at their respective vapor pressures and for components in the gas mixture (ϕ_i) at P, T in equilibrium with the liquid mixture.

2. The three-term Redlich-Kister equation can be used to describe the composition dependence of the liquid-phase activity coefficients at the reference pressure (P^r) on an isotherm at temperature T. Reference pressure was taken as zero in this work.

3. The pure-component isothermal compressibilities (β_i) are not functions of pressure and may be taken as those for the pure saturated liquids.

4. The excess volume (V^E) for the liquid mixture is not a function of pressure and may be taken as the value for the saturated liquid mixture.

5. The composition dependence of the saturated liquid mixture V^E can be approximated by a one-term Redlich-Kister equation on any isotherm.

With these assumptions the equations are

$$\ln\phi_i = \frac{2}{V}(y_i B_{ii} + y_j B_{ij}) - \ln Z \qquad \text{(A3)}$$

$$Z = \frac{PV}{RT} = 1 + \frac{B}{V} \qquad \text{(A4)}$$

$$B = \sum_{i=1}^{2} \sum_{j=1}^{2} y_i y_j B_{ij} \qquad \text{(A5)}$$

$$\ln\phi^s{}_i = \frac{2B_{ii}}{V^s{}_i} - \ln Z^s{}_i \qquad \text{(A6)}$$

$$Z^s{}_i = \frac{P^s{}_i V^s{}_i}{RT} = 1 + \frac{B_{ii}}{V^s{}_i} \qquad \text{(A7)}$$

$$(G^E)^{(P^r)} = x_1 x_2 [A' + B'(x_1 - x_2) + C'(x_1 - x_2)^2] \qquad \text{(A8)}$$

$$RT \ln \gamma_1^{(P^r)} = a_1 x^2{}_2 + b_1 x^3{}_2 + c_1 x^4{}_2 \qquad \text{(A9)}$$

$$RT \ln \gamma_2^{(P^r)} = a_2 x^2{}_1 + b_2 x^3{}_1 + c_2 x^4{}_1 \qquad \text{(A10)}$$

$$\begin{aligned} a_1 &= A' + 3B' + 5C' \\ a_2 &= A' - 3B' + 5C' \\ b_1 &= -4(B' + 4C') \\ b_2 &= 4(B' - 4C') \\ c_1 &= c_2 = 12C' \end{aligned} \qquad \text{(A11)}$$

$$\int_{P^s{}_i}^{P} V_i dP = V^s{}_i (P - P^s{}_i) - \frac{\beta^s{}_i V^s{}_i (P - P^s{}_i)^2}{2} \qquad \text{(A12)}$$

$$V^E = A'' x_1 x_2 \qquad \text{(A13)}$$

$$\int_{P^r}^{P} (\overline{V}_i - V_i) dP = A'' x^2{}_j (P - P^r) \qquad \text{(A14)}$$

A brief discussion of the assumptions will follow. For maximum accuracy of derived G^E values, third virial coefficient terms should have been included at temperatures near 170 K. There is no experimental information regarding ethane or cross third virials at temperatures this low, thus, no third virial terms were used. As long as the same truncated virial equation is used in calculating liquid-vapor equilibria as was used in developing the empirical liquid activity-coefficient equations, no significant uncertainties should have been introduced from this source.

The assumptions regarding representation of the composition dependence of the activity coefficients and the

non-pressure-dependent behavior of liquid isothermal compressibilities and excess volume should be quite satisfactory. It is known that the dependence of the liquid-mixture excess volume on composition is somewhat asymmetrical at temperatures below 135 K. However, the V^E term in the phase-equilibria equations is completely insignificant below 140 K, and there are no data above this temperature. It was decided that the uncertainties in extrapolating the available data would be larger than any errors involved with neglecting asymmetry. The V^E term is not of great importance, even at 172 K, and little error should have been introduced through use of the extrapolated V^E values.

Detailed Barker-Method Procedure

1. Input data: T, P^r, V^s_1, V^s_2, β^s_1, β^s_2, B_{11}, B_{22}, B_{12}, A'', initial guess for A′, and x_1-P-y_2 for each data point (including $x_1 = 0, 1$).

2. Calculate V^E, $\overline{V}_1 - V_1$ and $\overline{V}_2 - V_2$ for all liquid compositions using equations (A13) and (A14).

3. Calculate ϕ^s_1 and ϕ^s_2 using equations (A6) and (A7).

4. Calculate initial gas phase compositions as $y_1 = P^s_1 x_1/P$, $y_2 = P^s_2 x_2/P$ for a data point (x_1).

5. Calculate the activity coefficients $\gamma_1^{(0)}$ and $\gamma_2^{(0)}$ from equations (A9), (A10) and (A11) for the data point (x_1).

6. Calculate ϕ_1 and ϕ_2 using equations (A3), (A4) and (A5) for the data point (x_1).

7. Solve the phase equilibrium equation (A1) for y_1 and y_2 (they are *not* forced to sum to 1.0).

8. Iterate back through 6 until y_1 and y_2 have separately converged (they still need *not* add to 1.0).

9. Calculate $P = Py_1 + Py_2$.

10. Iterate back through 4 until all x_1's have been processed.

11. Increment A', B' and C' by solving the normal equations resulting from the least-squares procedure.

12. Iterate back through 4, reprocessing all data points on each iteration, until A', B' and C' separately converge.

13. Calculate standard deviations in A', B' and C' from the variance-covariance matrix resulting from the inverse of the normal matrix.

14. Print out results: A', B', C', $\sigma(A')$, $\sigma(B')$, $\sigma(C')$, $P(x_1)$, $y_1(x_1)$, $y_2(x_1)$, $\gamma_1^{(0)}(x_1)$, $\gamma_2^{(0)}(x_1)$, $\phi_1(x_1)$, $\phi_2(x_1)$, $G^{E(0)}(x_1)$.

Data Sources

Reference 22: B_{11}, V^s_1, β^s_1 and P^s_1 (only where P^s_1 was not reported with the phase-equilibria data).

Reference 23: V^s_2, β^s_2 and P^s_2 (where P^s_2 was not reported with the phase-equilibria data).

Reference 39: B_{22} and B_{12}, using $T_{c_2} = 305.50$ K, $V_{c_2} = 141.72$ cm³/mol, $T_{c_{12}} = 241.28$ K, $V_{c_{12}} = 119.65$ cm³/mol

Reference 38: T, K	A'', cm³/mol	
110	−2.2	
130	−3.7	
150	−6.4	
160	−8.0	extrapolated
170	−13.5	

Appendix B. Calculational Methods Used for Data Above 172 K

Orthogonal Collocation

The orthogonal collocation method using the unsymmetric convention was exactly as described by Christiansen and Fredenslund [21]. Orthogonal collocation is a numerical technique which is used to integrate along the saturated liquid mixture curve the partial differential coexistence equation resulting directly from the Gibbs-Duhem equation. P-x data along isotherms were processed to determine Henry's constants (H_{12}) and vapor-phase compositions (y) in the present work.

The computer program was obtained directly from the reference [21] authors. Input data, other than T-P-x data, included pure-component critical properties, acentric factors and Redlich-Kwong constants, as well as a binary parameter for deviation from the geometric-mean mixing rule for critical temperatures (k_{12}) and binary correlating parameters for mixture critical temperatures ($T_{c_{12}}$) and critical volumes ($V_{c_{12}}$). All of these data were taken directly from reference [29].

All collocation results reported here were calculated using 14 collocation points. Only minor differences in results were found with 8 to 14 collocation points for nearly all of the experimental isotherms.

Henry's Law Graphical Method

The calculational method was exactly as described under the section "Determination of Henry's Constants" in an article by Gunn, Yamada and Whitman [27]. This method utilized the unsymmetric form of the phase-equilibrium relation with a Van Laar equation to describe liquid-phase activity coefficients and a truncated virial equation for gas-phase nonidealities.

The computer program was obtained directly from the above authors [27]. Only T-P-x-y data from the liquid-vapor equilibria references were required as input. Data points were included only for methane mole fractions less than 0.5.

Correlations in the program yielded the virial coefficients, vapor pressures and liquid volumetric data necessary to perform the Henry's law analysis. The vapor pressures were found to be within 0.3% of those listed in references [22] and [23]. Liquid volumes from the program were close enough to known values so that errors from this source would be small.

Appendix C. Liquid-Vapor Equilibria With the Peng-Robinson Equation of State

Peng and Robinson [32] have proposed a modified Van der Waals equation of state for the calculation of thermodynamic properties. The development of the equation and its applications may be found in the original reference.

For this work, the equation was applied to the methane + ethane system in the following manner.

1. The value of the constant "b" in the equation was determined as proposed by Peng and Robinson [32].

2. The values of the constant "a" in the equation were obtained for both methane and ethane by determining the value of "a" such that the relation $f^L = f^V$ is satisfied at all points along the vapor pressure curves of both pure methane and ethane. The results obtained differ by $< 1\%$ from the values obtained using the correlation proposed in [32], thus the original correlation was used in all work reported here.

3. The mixing rules used were:

$$a = y^2_1 a_1 + 2y_1 y_2 a_{12} + y^2_2 a_2$$

$$a_{12} = (a_1 a_2)^{1/2} (b^2_{12}/b_1 b_2)^{1/2} (1 - k_{12})$$

$$b = y^2_1 b_1 + 2y_1 y_2 b_{12} + y^2_2 b_2$$

$$b_{12} = \left[\left(\frac{b_1^{1/3} + b_2^{1/3}}{2} \right) (1 + j_{12}) \right]^3$$

The same relations were used in the liquid phase. These mixing rules are not those proposed in the original reference.

4. The optimum values of j_{12} and k_{12} were obtained by applying a minimization technique proposed by Powell [40] to selected isotherms. For each isotherm, the values of j_{12} and k_{12} were determined to minimize the value

$$\Sigma \left[\frac{|x_{exp} - x_{calc}| + |y_{exp} - y_{calc}|}{2(\text{number of data points})} \right].$$

5. Overall values for j_{12} and k_{12} of 0.0066 and 0.025 respectively, were then obtained by using a weighted average based on the number of data points for each isotherm. Analysis of interaction virial coefficient (B_{12}) data for the temperature region 273 to 323 K [41–43] produces k_{12} values ranging from 0.004 to 0.019.